Analysis of Constant Tension-Induced Rupture of Lipid Membranes Using Activation Energy

Analysis of Constant Tension-Induced Rupture of Lipid Membranes Using Activation Energy

Mohammad Abu Sayem Karal,[a,] *Victor Levadnyy,*[b] *and Masahito Yamazaki* [a,c,d,]*

[a] Integrated Bioscience Section, Graduate School of Science and Technology, Shizuoka University, Shizuoka 422-8529, Japan, [b] Theoretical Problem Center of Physico-Chemical Pharmacology, Russian Academy of Sciences, Kosugina, 4, 117977, Moscow, Russia, [c] Nanomaterials Research Division, Research Institute of Electronics, Shizuoka University, Shizuoka 422-8529, Japan, [d] Department of Physics, Faculty of Science, Shizuoka University, Shizuoka 422-8529, Japan.

Corresponding Author:

Dr. Masahito Yamazaki

Nanomaterials Research Division, Research Institute of Electronics,

Shizuoka University, 836 Oya, Suruga-ku, Shizuoka 422-8529, Japan

Tel / Fax: 81-54-238-4741; E-mail: yamazaki.masahito@shizuoka.ac.jp

ABSTRACT

The stretching of biomembranes and lipid membranes plays important roles in various physiological and physicochemical phenomena. Here we analyzed the rate constant k_p of constant tension-induced rupture of giant unilamellar vesicles (GUVs) as a function of tension σ using its activation energy U_a. To determine the values of k_p, we applied constant tension to a GUV membrane using the micropipette aspiration method and observed rupture of GUVs, then analyzed these data statistically. First, we investigated the temperature dependence of k_p for GUVs of charged lipid membranes composed of negatively charged dioleoylphosphatidylglycerol (DOPG) and electrically neutral dioleoylphosphatidylcholine (DOPC), By analyzing this result, the values of U_a of tension-induced rupture of DOPG/DOPC-GUVs were obtained. U_a decreased with an increase in σ, supporting the classical theory of the tension-induced pore formation. The analysis of the relationship between U_a and σ using the theory on the electrostatic interaction effects on the tension-induced rupture of GUVs provided the equation of U_a including electrostatic interaction effects, which well fit the experimental data of the tension dependence of U_a. A constant which does not depend on tension, U_0, was also found to contribute significantly to U_a. The Arrhenius equations for k_p using the equation of U_a and the parameters determined by the above analysis fit well to the experimental data of the tension dependence of k_p for DOPG/DOPC-GUVs as well as for DOPC-GUVs. On the basis of these results, we discussed the possible elementary processes underlying the tension-induced rupture of GUVs of lipid membranes. These results indicate that the Arrhenius equation using the experimentally determined U_a is useful in the analysis of tension–induced rupture of GUVs.

Table of Content

Experimentally determined activation energy explains the tension dependence of rate constant of tension-induced rupture of charged and neutral lipid membranes.

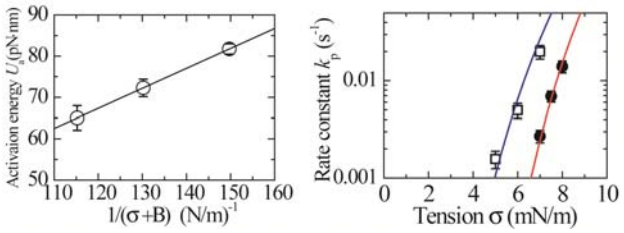

Lists of symbols

A_F : pre-exponential factor

A_0 : cross-sectional area per lipid molecule in the bilayer

a : an adjustable parameter defined by $a = \Omega_p/\Omega$ ($0 \le a \le 1$)

B : a term in $U(r, \sigma)$, which is due to electrostatic interactions arising from surface charges

D : diameter of the spherical portion of the GUV exterior to the micropipette

D_r : diffusion coefficient of the particle in r-phase space

d : internal diameter of the micropipette

k_p : rate constant of GUV rupture (or rate constant of tension-induced pore formation)

$P_{intact}(t)$: fraction of intact (un-ruptured) GUVs among all the GUVs

ΔP : difference in pressure between the outside and the inside of a micropipette

R^2 : coefficient of determination

r : radius of a pre-pore

r_c : critical radius

T : absolute temperature

U_a : activation energy of tension-induced rupture of a GUV

$U(r, \sigma)$: total free energy of a pre-pore

U_0 : a constant term in $U(r, \sigma)$, which does not depend on tension

X : DOPG molar fraction in the lipid membrane

σ : tension in the lipid membrane

Γ : line tension (or the line free energy per unit length) of the pre-pore edge in lipid membranes

Ω : surface charge density of the membrane

Ω_p : surface charge density on the pre-pore wall

$1/\kappa$: Debye length

λ_B : Bjerrum length in water

ε_w : relative dielectric constant of water

ε_0 : permittivity of free space

τ : the lifetime of the intact GUV

1. Introduction

When various external forces are applied to cells and vesicles, lateral tension is induced in the membranes and concomitantly stretching of the membranes occurs. It is well known that many kinds of physiological and physicochemical phenomena are induced or controlled by the stretching of membranes. For example, mechano-sensitive channels open when plasma membranes are stretched.[1-3] In the case of applied external forces, if the tension is enough large, pore formation starts to occur in the membranes, resulting in cell death or rupture of the vesicles.[4-6] Antimicrobial peptides also induce the stretching of lipid membranes, causing pore formation.[7,8] It is therefore important to elucidate the mechanism of tension-induced pore formation and the effect of tension on the physicochemical properties of lipid membranes. Giant unilamellar vesicles (GUVs) composed of lipid membranes have been used to elucidate the kinetics and mechanism of tension-induced pore formation in lipid membranes and rupture of the vesicles.[4-6,9-13]

According to the classical theory of tension-induced pore formation in soft films,[14-16] once such a pre-pore is formed in the membrane, the total free energy of the system changes by an additional free energy [called the free energy of a pre-pore, $U(r, \sigma)$], which consists of two terms: one term ($-\pi r^2\sigma$) is due to the lateral tension, σ, favoring expansion of the pre-pore, and the other term ($2\pi r\Gamma$) is due to the line tension of the pre-pore edge, Γ (i.e., the line free energy per unit length of a pre-pore in a lipid membrane), favoring closure of the pre-pore. The maximum of $U(r, \sigma)$ is $U_{max} = \pi\Gamma^2/\sigma$ at the critical radius $r = r_c$ ($= \Gamma/\sigma$). If the radius of a pre-pore is less than r_c, it closes quickly. However, if the radius reaches r_c, the pre-pore transforms into a pore and the radius becomes infinity, i.e., the rupture of the GUV occurs. Therefore, U_{max} works as the energy barrier for the pore formation and the GUV rupture. In the case of constant tension-induced rupture of a GUV, the radius of a pre-pore reaches r_c stochastically and hence rupture occurs stochastically, whose analysis provided the rate constant of tension-induced rupture of a GUV.[11,13] It is worth to note that U_{max} works as the activation energy (U_a) of tension-induced rupture of GUVs. We previously

determined experimentally the U_a of tension-induced rupture of GUVs composed of electrically neutral lipid membranes. By analyzing these data, we obtained $U_a = U_0 + \pi\Gamma^2/\sigma$, where U_0 is a constant, and proposed that U_0 represents the nucleation free energy required to form a hydrophilic pre-pore.[17]

In this report, we analyzed the tension dependence of the rate constant k_p of constant tension-induced rupture of a GUV using the experimentally determined U_a. First, we investigated the temperature dependence of k_p for GUVs of charged lipid membranes composed of negatively charged dioleoylphosphatidylglycerol (DOPG) and neutral dioleoylphosphatidylcholine (DOPC). By analyzing this data, we obtained the U_a values of constant tension-induced rupture of DOPG/DOPC-GUVs. Then we analyzed the experimental relationship between U_a and σ by comparing with the theoretical equation of U_a developed by us recently.[13] Next, to elucidate the validity of the equation of U_a, we compared the Arrhenius equation for k_p using the experimentally determined U_a with the data of the tension dependence of k_p for the charged DOPG/DOPC and the neutral DOPC membranes. Finally we discussed the possible elementary processes underlying tension-induced rupture of the GUVs.

2. Materials and Methods

DOPG and DOPC were purchased from Avanti Polar Lipids Inc. (Alabaster, AL). Bovine serum albumin (BSA) (crystallized), NaCl (JIS special grade), sucrose (JIS special grade), and glucose (JIS special grade) were purchased from Wako Pure Chemical Industries Ltd. (Osaka, Japan). Piperazine-1,4-bis(2-ethanesulfonic acid) (PIPES) and O,O'-Bis(2-aminoethyl)ethyleneglycol-N,N,N',N',-tetraacetic acid (EGTA) were purchased from Dojindo Laboratory (Kumamoto, Japan). All these reagents were used without purification. 40%DOPG/60%DOPC-GUVs (where % indicates mol%) were prepared in buffer A (10 mM PIPES, pH 7.0, 150 mM NaCl, 1.0 mM EGTA).[11] To purify these GUV suspensions, the membrane filtering method was used;[18] after centrifugation, the supernatant was filtered through a nuclepore membrane with 10 μm diameter pores (Whatman, GE Healthcare, UK, Ltd., Buckinghamshire, England) in buffer A containing 0.10 M glucose for 1.0 h at a flow rate of 1.0 mL/min at room temperature (20–25 °C), and the suspension which was not passed through the filter was collected and used for following experiments as a purified GUV suspension. The purified GUV suspension (300 μL) (0.10 M sucrose in buffer as the internal solution; 0.10 M glucose in buffer as the external solution) was transferred into a hand-made microchamber, which had

been formed on a glass slide by inserting a U-shaped silicone-rubber spacer,[19] GUVs were observed using an inverted fluorescence, phase-contrast and differential interference contrast (DIC) microscope (IX-71, Olympus, Tokyo, Japan) at various temperatures controlled via a stage thermocontrol system (ThermoPlate CBU, TP-CH110R-C, Tokai Hit, Shizuoka, Japan).[11] Phase-contrast and DIC images of GUVs were recorded using a charge-coupled device (CCD) camera (CS230B, Olympus).

The rate constant k_p of GUV rupture was determined using the method of Levadny et al.[11] To apply tension, σ, to the lipid membranes of single GUVs, we used the micropipette aspiration method.[20] σ can be described as a function of the difference in pressure between the outside and the inside of a micropipette, ΔP:[20]

$$\sigma = \frac{\Delta P d}{4(1 - d / D)}, \qquad (1)$$

where d represents the internal diameter of the micropipette and D represents the diameter of the spherical portion of the GUV exterior to the micropipette. The measurement of ΔP was done using a differential pressure transducer (DP15, Validyne, CA), pressure amplifier (PA501, Validyne, CA), and a digital multimeter.[19] Glass micropipettes were prepared by pulling 1.0 mm glass capillary composed of borosilicate glass (G-1, Narishige, Tokyo, Japan) using a puller (PC-10, Narishige, Tokyo, Japan).[19] Micropipettes were coated with 0.50 % (w/v) BSA in 0.10 M glucose, and glass surfaces in chambers were coated with 0.10 % (w/v) BSA in 0.10 M glucose. Here we used BSA coating on the glass surface to prevent strong adhesion of lipid membranes of GUVs to the glass surface.

3. Results

The temperature dependence of k_p of 40%DOPG/60%DOPC-GUV rupture was measured. First, a constant tension of 7.0 mN/m was applied to a GUV membrane at 12 °C in buffer A containing 0.10 M glucose using a micropipette until the GUV ruptured. A single GUV was held at the tip of a micropipette for 2 min using only slight aspiration pressure, providing a tension of ~0.5 mN/m on the GUV membrane. The pressure difference, ΔP, was then rapidly (~10 s) increased to obtain a specific level of tension, σ (here, σ = 7.0 mN/m), which was maintained. After 237 s, the GUV was suddenly aspirated into the micropipette. Based on previous papers,[5,7,10,11] this event can be explained as follows. First, a pore was formed in the GUV

membrane, causing the rupture of the GUV, and then the GUV was completely aspirated into the micropipette due to the pressure difference between the inside and the outside of the micropipette. The time of rupture of a GUV was defined as the time at which the GUV was completely aspirated, and was recorded with a resolution of less than 1 s. Repetition of this experiment with 20 single GUVs (n = 20) showed that rupture of a GUV occurred stochastically. The time course of the fraction of intact (un-ruptured) GUVs among all the GUVs, $P_{\text{intact}}(t)$, was fit to a single exponential decay function (○ in Fig. 1A):

$$P_{\text{intact}}(t) = \exp\left(-k_{\text{p}}t\right), \tag{2}$$

where k_{p} is the rate constant of GUV rupture, which is the same as the rate constant of tension-induced pore formation, t represents the duration of the tension applied to the GUV (i.e., the application of the tension was started at t = 0). This fitting provided a k_{p} value of 6.3×10^{-3} s^{-1}.

The same experiment using σ = 7.0 mN/m was then performed at different temperatures (i.e., 18 °C and 25 °C) (n = 20 for each temperature). The decrease in $P_{\text{intact}}(t)$ occurred more rapidly with an increase in temperature (Fig. 1A), and the value for k_{p} obtained from curve fitting was 8.8×10^{-3} s^{-1} at 18 °C and 1.4×10^{-2} s^{-1} at 25 °C. We made the same experiments three times to obtain the mean values and the standard errors of k_{p} (Table 1). To obtain the activation energy, U_{a}, of GUV rupture, we plotted ln k_{p} vs. $1/T$ (○ in Fig. 1B). The value of U_{a}, was obtained from the slope of the resulting linear fit: U_{a} = 65 ± 3 pN·nm (= 15.8 ± 0.7 kT, where k represents the Boltzmann constant and T = 298 K).

The temperature dependence of k_{p} was measured using tensions of 5.0 and 6.0 mN/m (Table 1). Fig. 1B shows the plots of ln k_{p} versus $1/T$ for these data. These plots are linear, and values for U_{a} were determined from the corresponding slopes: U_{a} = 82 ± 1 pN·nm for σ = 5.0 mN/m, and U_{a} = 72 ± 2 pN·nm for σ = 6.0 mN/m.

For charged membranes such as DOPG/DOPC membranes considered here, the effects of electrostatic interactions on tension-induced rupture has to be taken into account.[13] We assumed that the structure of a hydrophilic pre-pore is the same as that of a pore, although there is no experimental evidence on the structure of pre-pores. Recent studies using molecular dynamics (MD) simulations indicate that pores in the lipid membranes have a toroidal structure, in which the outer and inner monolayers bend and merge in a pore with

an inner wall composed of lipid head groups.[21,22] Therefore, we consider here that a hydrophilic pre-pore has a toroidal structure. Hence, the surface of its wall is charged due to presence of the charged lipid head groups. Therefore, the total free energy of a pre-pore $U(r, \sigma)$ has to include the proper electrostatic term, U_{el},[13]

$$U(r,\sigma) = 2\pi\Gamma r - \pi\sigma r^2 + U_{el}(r, X, \kappa). \quad (3)$$

Generally, the electrostatic interactions in biomembranes or lipid membranes in aqueous solution are determined by the surface charge density of the membrane, Ω, and salt concentration in the solution, which effect is described by the Debye length, $1/\kappa$.[23,24] Various physiological phenomena are reasonably explained by these electrostatic interactions.[25-28] Here, Ω of DOPG/DOPC membranes equals $-eX/A_0$, where e is the elementary charge, X is the DOPG molar fraction in the lipid membrane, and A_0 is the cross-sectional area per lipid molecule in the bilayer under no tension (here we assume that A_0 of a DOPG molecule is the same as A_0 of DOPC (= 72.5 Å^2)).[29] For simplicity, we also assume that the structure of the pre-pore is a cylinder with radius r and height h (= bilayer thickness = 4.0 nm) and the surface (i.e., the wall) of the cylinder is composed of head groups of lipids (DOPG and DOPC). This simplification is necessary to obtain an analytical solution of Poisson-Boltzmann equation for the analysis of the electrostatic interaction effects inside the pre-pore (see the details later). For generalization, we assume that the surface charge density on the pre-pore wall, Ω_p, is less than that of the GUV surface and hence $\Omega_p = a\Omega$ (where a is an adjustable parameter ($0 \le a \le 1$), and that Ω_p (i.e., a) does not depend on the pre-pore radius. The existence of a double electric layer (DEL) near the membrane surface is the main difference between charged and neutral GUVs.[23,24] The appearance of a pre-pore in a charged GUV has two consequences.[30,31] One is a reduction or disappearance of the DEL above the pre-pore, which decreases the total free energy of the system. The other is the appearance of the DEL inside the pre-pore, which is filled with solution. These consequences change the total free energy of system. We obtained the electrostatic Gibbs free energy density (per unit of area of the membrane) of the DEL as follows;[13] to obtain the free energy density of the DEL above the GUV membrane surface, we used Lekkerkerker's equation,[32] and to obtain the free energy density of the DEL inside the pre-pore, we used a linearized Poisson-Boltzmann equation for cylindrical symmetry. Hence, the total free energy of a pre-pore with radius of r in a charged GUV, $U(r, \sigma, B)$, is obtained as follows:[13]

$$U(r,\sigma,B) = 2\pi\Gamma r - \pi r^2(\sigma + B), \quad (4)$$

where B is a term due to electrostatic interactions arising from surface charges. B can be written as:

$$B = \left\{ 4\Omega \left[\frac{1-q}{p} + \ln(p+q) \right] \frac{kT}{e} - \frac{\Omega^2}{\varepsilon_w \varepsilon_0} a^2 \frac{h}{2} \right\}, \quad (5)$$

where ε_w is the relative dielectric constant of water, ε_0 is the permittivity of free space, $p = 2\pi\lambda_B X / \kappa A_0$ and $q = \sqrt{1+p^2}$, and λ_B is the Bjerrum length in water, $\lambda_B = e^2 / 4\pi kT\varepsilon_0\varepsilon_W$ (= 0.716 nm at 25 °C). To explain the experimental result that k_p of 40%DOPG/60%DOPC-GUVs is larger than that of DOPC-GUV,[11] the condition $B > 0$ must be satisfied, which corresponds to $a \leq 0.56$. Eq. 4 indicates that $U(r, \sigma, B)$ has a maximum of $\pi\Gamma^2/(\sigma + B)$ at $r_c = \Gamma/(\sigma + B)$, which is the barrier of the free energy. On the other hand, the experimental data for U_a vs. $1/(\sigma + B)$ at 25 °C fit a linear line expressed by $U_a = U_0 + C/(\sigma + B)$, where U_0 and C are constants (Fig. 2). Therefore, we consider the following revised equation:

$$U_a = U_0 + \pi\Gamma^2 / (\sigma + B) . \quad (6)$$

We consider that U_0 has the same physical meaning as that in the activation energy of the tension-induced rupture of DOPC-GUV,[17] i.e., the nucleation free energy required to form a hydrophilic pre-pore. Using eq. 6, we obtained the best fit data at $a = 0.49$, which corresponds to $B = 1.8$ mN/m, where $U_0 = 9.0 \pm 0.4$ pN·nm (= 2.2 ± 0.1 kT), $\Gamma = 12.4 \pm 0.2$ pN. We also obtained good fits for $0.45 \leq a \leq 0.56$, which corresponds to $0.2 \leq B \leq 2.6$ mN/m (Table 2). However, for $a \leq 0.44$, U_0 becomes negative, and hence this condition was excluded because U_0 should be positive based on its physical meaning.

Generally, the rate constant for any reactions and structural transitions can be described by the Arrhenius equation using their activation energies. Using eq. 6, the Arrhenius equation for k_p can be written as

$$\begin{aligned} k_P &= A_F \exp(-U_a / kT) \\ &= A_F \exp\left(\frac{-U_0}{kT}\right) \exp\left[\frac{-\pi\Gamma^2}{kT(\sigma + B)} \right], \end{aligned} \quad (7)$$

where A_F is the pre-exponential factor, which has a meaning of the frequency factor. Using the above values ($U_0 = 9.0$ pN·nm, $\Gamma = 12.4$ pN, $a = 0.49$ (i.e., $B = 1.8$ mN/m)) and eq. 7, we fit the data of the tension dependence of k_p for 40%DOPG/60%DOPC-GUVs in buffer A at 25 °C from ref. 11. In Fig. 3, the solid

blue line shows the best-fit curve using a parameter $A_F = 5.0 \times 10^4\ s^{-1}$. Good fittings were also obtained for a = 0.47 – 0.51 (i.e., B = 1.3 – 2.2 mN/m), judging from the coefficient of determination, R^2 values (> 0.90) (Table S1 in Supporting Information). We therefore obtained the optimum values of the parameters: U_0 = 5–12 pN·nm, Γ = 12–13 pN, and $A_F = (5.0–15) \times 10^4\ s^{-1}$. Applying the same method, the data of DOPC-GUV in ref. 11 were fit well using the values (U_0 = 19 pN·nm, Γ = 11.6 pN)[17] and eq. 7 (B = 0). The solid red line in Fig. 3 shows the best-fit curve using the parameter $A_F = 6.3 \times 10^5\ s^{-1}$.

4. Discussion

In this report, first we investigated the temperature dependence of tension-induced rupture of 40%DOPG/60%DOPC-GUVs. In our experiments, we just observed the aspiration of a GUV during the application of constant tension to the GUV membrane by a micropipette. As described in the result section, it is reasonably consider that rupture of a GUV induces its aspiration into the micropipette. Generally, several causes for the rupture of a GUV can be considered. In this connection, it is worth to note that Brochard-Wyart et al. observed a large pore in a GUV membrane which was stretched as a result of intense optical illumination, and analyzed the fast dynamics of pore closings in the GUV membrane.[4,9] Based on this result, we can reasonably consider that stretching due to tension induces a pore in a membrane. Therefore, we consider that in our experiments at first a pore was formed in the GUV membrane, causing the rupture of the GUV, and then the GUV was completely aspirated into the micropipette due to the pressure difference between the inside and the outside of the micropipette. Evans et al. investigated the rupture of a GUV under dynamic applied tension, in which ramps of tension with loading rates (i.e., tension/time) were applied using a micropipette, and interpreted the rupture occurred due to the tension-induced pore formation.[5,10] As described in the result section, the aspiration of a GUV occurred rapidly (less than 1 s) and therefore it is difficult to discriminate the pore formation from the aspiration of the GUV. k_p values were determined as the rate constants of the constant tension-induced rupture of a GUV, which are the same as the rate constants of tension-induced pore formation in the GUV membrane. On the basis of these discussions, we can reasonably consider that we obtained the temperature dependence of the rate constant of the tension-induced pore formation in 40%DOPG/60%DOPC-GUVs in this report. Then, from these data we determined U_a of the tension-induced pore formation.

The experimental results clearly indicate that U_a decreased with an increase in tension σ. This result supports the classical theory of the tension-induced pore formation described in the Introduction. The analysis of the relationship between U_a and σ using the theory on the electrostatic interaction effects on the tension-induced rupture of GUVs[13] provided the equation $U_a = U_0 + \pi\Gamma^2/(\sigma + B)$, where U_0 is a constant. The experimental data of the tension dependence of U_a (Fig. 2) was well fit to this equation and from this fitting probable values for U_0, Γ, and a were obtained. This result supports the validity of the theory. Finally, we found that the Arrhenius equation for k_p using the equation of U_a and the parameters determined by the analysis of U_a vs. $1/(\sigma + B)$ fit well to the experimental data of the tension dependence of k_p (Fig. 3) for the charged DOPG/DOPC-GUVs and the electrically neutral DOPC-GUVs. In this case, A_F is the single adjustable parameter, whose optimal values were determined by this fitting. These results indicate that the Arrhenius equation using the experimentally determined U_a is useful in the analysis of tension–induced rupture of GUVs.

When we analyzed the effect of the electrostatic interaction on the total free energy of a pre-pore $U(r, \sigma)$ theoretically in our previous paper,[13] to obtain an analytical solution of Poisson-Boltzmann equation we approximated the toroidal structure of a pre-pore as the cylindrical structure and assumed the surface charge density on a pre-pore wall, Ω_p, does not depend on the radius of the pre-pore. However, it turned out that the equation of the activation energy U_a (eq. 6) derived based on these approximation and assumption well fit the experimental data (Fig. 2). Moreover, the Arrhenius equation for k_p using the equation of U_a provided a good fit to the independent experimental data of the tension dependence of k_p (Fig. 3). Therefore, we consider that these approximation and assumption are good as the first trial. However, in future, we need further analysis using a structural model similar to the toroidal structure and examine the validity of the assumption.

The physical meaning of the parameter B is the tension due to the electrostatic interactions judging from eqs. 4 and 5. Table 2 summarizes the values of B at 25 °C which provide good fittings in Fig. 2. At 25 °C the best fitting in Fig. 2 was obtained at a = 0.49. As indicated by eq. 5, the B values weekly depend on temperature if a has the same value (Table 3). We estimated the values of U_a for each temperature by eq. 6 using these B values and the best fit parameters (a = 0.49, U_0 = 9.0 pN·nm, Γ = 12.4 pN) (Table 3). The variations of U_a over temperature in the measurements were 3–4 % of U_a at the lowest temperature for each

tension. Based on this result, we assumed that the U_a value is constant over the temperature ranges used in the experiments shown in Fig. 1B. This assumption was correct within the experimental errors. Hence, we were able to obtain the U_a values from the analysis of Fig. 1B.

In the experiments shown in Fig. 1B. Fig. 2, and Fig. 3, the numbers of the data points are only 3. This limited number of the data points may decrease the accuracy of the analysis. There are several reasons for it. One is that the measurable region of k_p is limited for 0.001–0.02 s^{-1} in the present experimental method developed by us.[11] The other is the limited temperature range of the experiments of the tension-induced rupture of GUVs (i.e., 10–37 °C), because at higher temperatures the rate of water evaporation from the chamber containing the GUVs is high, which could induce osmotic pressure on the GUVs and hence affect the values of k_p significantly. In future we will improve this methodology to obtain more data point.

Now we discuss the elementary processes underlying tension-induced rupture or pore formation in lipid membranes. At present we don't have sufficient experimental evidence on the pre-pores, and hence here we describe our hypothesis on the structures and the evolution of a pre-pore into a pore. The results in this report indicate that the activation energy of tension-induced rupture, U_a, is composed of the constant, U_0, and the free energy barrier of the hydrophilic pre-pore ($= \pi\Gamma^2/(\sigma + B)$) (eq. 6). We consider that U_0 represents the nucleation free energy required to form a hydrophilic pre-pore. However, currently the process of the formation of the hydrophilic pre-pore is controversial. Lipid membranes are self-assemblies of many lipid molecules due to a week hydrophobic interaction. Therefore, thermal fluctuations of the lateral density of lipids (i.e., rarefaction and condensation) exist in the membrane, and hence we can expect that various structures of rarefactions appear transiently in the membranes. As one of these rarefactions, a hydrophobic pre-pore whose wall contacting water is mainly composed of the hydrocarbon chains of lipid molecules was proposed earlier.[33] However, according to the recent MD simulation studies,[21] such a hydrophobic pre-pore was not formed before the formation of the hydrophilic pre-pore. When the size of a rarefaction reaches a critical value, it becomes a hydrophilic pre-pore with the toroidal structure whose wall contacting water is mainly composed of the hydrophilic segments of lipid molecules (Fig. 4A (1)).[6,20,33-35] As the radius of the pre-pore increases, the radius of water channel at the center of the pre-pore increases (Fig. 4A (2)). We can reasonably consider that U_0 is the free energy of a state I between a hydrophobic rarefaction (or pre-pore) and a hydrophilic pre-pore at $r = r_0$ (Fig. 4A (1)), because U_0 is a nucleation free energy required to form a

hydrophilic pre-pore.[17] Here we use the definition of the radius of a hydrophilic pre-pore shown in Fig. 4A (2) because all the bending region of the membrane with deformation of lipid molecules contributes the line tension, Γ. If we use this definition, the free energy profile of the hydrophilic pre-pore as a function of r can be described by the following equation:

$$U(r,\sigma,B) = 2\pi\Gamma(r - r_0) - \pi(r^2 - r_0^2)(\sigma + B) + U_0 \qquad \text{for} \quad r \geq r_0 . \tag{8}$$

In eq. 8, $U(r, \sigma, B)$ has a maximum of $U_0 + \pi\Gamma^2/(\sigma + B) = U_a$ at $r = r_0 + r_c$, where $r_c = \Gamma/(\sigma + B)$, and $U(r, \sigma, B) = U_0$ at $r = r_0$ (Fig. 4B). The activation energy of the transition from state I to the pore state (state P) is $\pi\Gamma^2/(\sigma + B)$, since state I has a free energy of U_0. The total activation energy for the transition from the intact state with no pre-pore (i.e., state O) to state P can be described using eq. 6. We consider that the structure of the hydrophilic pre-pore is the same as that of a pore (i.e., the toroidal structure). However, the stabilities of the pre-pore and the pore are different; the pre-pore is unstable because when its radius is less than the critical radius (i. e., $r_0 + r_c$) in the free energy profile (Fig. 4B) the pre-pore closes quickly. In contrast, a pore cannot be closed and its radius becomes infinity (i.e., rupture of the GUV occurs) because its radius is larger than the critical radius in the free energy profile (Fig. 4B).

When we consider the rate of the transitions between different states and that of chemical reactions, we should take into account of only stable or metastable states which have a free energy minimum.[36] Hence, for the tension-induced rupture of a GUV, there are only three states; the state O (i.e., intact GUV with no pre-pores at $r = 0$), the state I (where a GUV membrane has a pre-pore with radius $r = r_0$), and the state P (where a membrane has a pore with $r = \infty$ or the state of ruptured GUV). Here, we assume that another stable state does not exist in the process of the rupture of the GUV. However, as we described in the Introduction, between these stable states there are many transient, unstable states containing various sizes of pre-pores and pores. As discussed in our previous paper,[17] we can consider two models for the process of the formation of a hydrophilic pre-pore: in model A,[5,33] there is an energy barrier between the state O and the state I (Fig. 5A), and in model B,[21] there is no energy barrier between the two states (Fig. 5B). In the model A, the state I is a metastable state. In contrast, in the model B there is no metastable state, which was supported by the MD simulation results.[21,34]

In our previous paper, we obtained the equation of k_p using mean first passage time (MFPT) approach, which reasonably explained the experimental results of tension dependence of k_p.[11,13] In this case we did not know the existence of U_0, and therefore we considered only single-step transition where an energy barrier exists at $r = r_c$. In this MFPT approach, evolution of a pre-pore is treated as a particle in stochastic motion in r-space within an asymmetric double-well potential $U(r)$ according to the Kramers theory of Brownian motion[37,38]. The walls with an infinite barrier at $r = 0$ and a limited barrier at $r = r_c$ work, respectively, as a reflecting boundary and an absorbing boundary. Then, the lifetime of the intact GUV, τ, is defined as the time when a particle arrives at $r = r_c$ and escapes from the hole, which is determined by the MFPT technique:[37-38.9]

$$\tau = \left(\frac{kT}{D_r}\right)\left[\frac{2\pi}{\sqrt{\partial^2 U(0)/\partial r^2 \left|\partial^2 U(r_c)/\partial r^2\right|}}\right] \exp\left[\frac{U_a}{kT}\right], \qquad (9),$$

where D_r is the diffusion coefficient of the particle in r-phase space. Applying this MFPT approach and the procedure commonly used for its simplification[39], one can obtain the rate constant $k_p = 1/\tau$ for the transition of energy barrier at $r = r_c$. Using the approximated $U(r)$ for $0 < r < r_c/2$ as $U(r) = 3\pi r^2(\sigma + B)$, we obtained[13]

$$k_p = k_p(\sigma, B) = \frac{1}{\tau} = \left(\frac{D_r\sqrt{3}}{kT}\right)(\sigma + B)\exp\left[-\frac{\pi\Gamma^2}{kT(\sigma + B)}\right]. \qquad (10)$$

However, here we recognize the presence of U_0 and the two-step transition involving the process of the formation of a hydrophilic pre-pore and the evolution of the hydrophilic pre-pore. Hence, at present stage, we cannot obtain k_p using the MFPT approach.

In our previous paper,[13] we analyzed only one kind of the data (i.e., k_p vs σ) using the MFPT approach with $U_0 = 0$ using eq. 10. Good fittings of eq. 10 to the experimental data were obtained in the wide regions of a (i.e., $0.1 \le a \le 0.49$) (Table S2), and hence we were unable to obtain the optimum values of a. In this case, the condition $a \le 0.49$ was obtained by $B > 0$, where the theory agreed with the experimental results that k_p increased with an increase in the electrostatic interactions. If we consider the physical meaning of B (i.e., the extra tension due to the electrostatic interactions), it is also clear that $B > 0$. In contrast, in this report,

we analyzed two kinds of experimental data (i.e., U_a vs $1/(\sigma + B)$ and k_p vs σ) for the fittings, and hence we found that good fittings of eq. 7 and 10 to the experimental data were obtained in the limited regions of a (i.e., $0.47 \leq a \leq 0.51$). The condition $B > 0$ must be satisfied, which corresponds to a ≤ 0.56, and the physical meaning of U_0 (i.e., $U_0 \geq 0$) required $0.45 \leq a$, and hence it turned out that we can consider only the region of $0.45 \leq a \leq 0.56$. The data of U_a vs $1/(\sigma + B)$ provides the relationship between a, U_a, and Γ, which decreased the region of the optimum values of a to fit the data of k_p vs σ. Therefore, we were able to determine the optimum values of a.

It is important to consider the relationship between the molecular structures or intermolecular interactions of lipid membranes and the constant tension-induced rupture of GUVs. In our theory (eq. 7), the values of three parameters (i.e., Γ, B, and U_0) reflects the molecular structures or intermolecular interactions of lipid membranes. It is reported that GUVs of lipid membranes with shorter hydrocarbon chains were ruptured at smaller tension,[5] which can be considered due to smaller Γ. In our previous paper,[13] it is shown that GUVs composed of charged lipids were ruptured at smaller tension, which was due to larger B. At present we do not know the relationship between U_0 and the molecular structures or the intermolecular interactions. Other intermolecular interactions such as hydrogen bonding[40] may play important roles in the tension-induced rupture of GUVs, but currently we do not know which parameter is affected by these intermolecular interactions. Further studies on the tension-induced rupture or pore formation are indispensable.

5. Conclusion

In this report, we determined U_a of tension–induced rupture of GUVs of the charged DOPG/DOPC membranes using the data of the temperature dependence of k_p. The analysis of the relationship between U_a and σ provided the equation of U_a. The Arrhenius equation for k_p using the equation of U_a and the parameters determined by the above fitting was fit well to the experimental data of k_p vs σ for the charged and the neutral membranes, which provided the optimal values of the parameters. Two kinds of experimental data (U_a vs σ and k_p vs σ) were used for the fitting and therefore a limited range of optimum values of the parameters were determined. These results indicate that the Arrhenius equation using experimentally determined U_a is useful in the analysis of tension–induced rupture of charged and neutral lipid membranes.

Acknowledgment: This work was supported in part by a Grant-in-Aid for Scientific Research (B) (No.15H04361) from the Japan Society for the Promotion of Science (JSPS) to M.Y.

References

1. F. Sachs, *Physiology*, 2010, **25**, 50-56.
2. S. I. Sukharev, P. Blount, B. Martinac, F. R. Blattner, C. Kung, *Nature*, 1994, **368**, 265-268.
3. N. Levina, S. Totemeyer, N. R. Stokes, P. Louis, M. A. Jones, I. R. Booth, *EMBO J.*, 1999, **18**, 1730-1737.
4. O. Sandre, L. Moreaux, F. Brochard-Wyard, *Proc. Natl. Acad. Sci. USA*. 1999, **96**, 10591-10596.
5. E. Evans, V. Heinrich, F. Ludwig, W. Rawicz, *Biophys. J*. 2003, **85**, 2342-2350.
6. G. Fuerties, D. Giménez, S. Esteban-Martin, O. L. Sánchez-Muñoz, J. Salgado, *Eur. Biophys. J.* 2011, **40**, 399-415.
7. M. A. S. Karal, J. M. Alam, T. Takahashi, V. Levadny, M. Yamazaki, *Langmuir*, 2015, **31**, 3391-3401.
8. M. Z. Islam, J. M. Alam, Y. Tamba, M. A. S. Karal, M. Yamazaki, *Phys. Chem. Chem. Phys*., 2014, **16**, 15752-15767.
9. E. Karatekin, O. Sandre, H. Guitouni, N. Borghi, P. –H. Puech, F. Brochard-Wyard, *Biophys. J.* 2003, **84**, 1734-1749.
10. E. Evans, B. A. Smith, *New J. Phys.* 2011, **13**, 095010.
11. V. Levadny, T. Tsuboi, M. Belaya, M. Yamazaki, *Langmuir*, 2013, **29**, 3848-3852.
12. I. Gozen, P. Dommersnes, *Eur. Phys. J*. 2014, **223**, 1813-1829.
13. M. A. S. Karal, V. Levadny, T. Tsuboi, M. Belaya, M. Yamazaki, *Phys. Rev. E.* 2015, **92**, 012708.
14. J. D. Litster, *Phys. Lett.* 1975, **53A**, 193-194.
15. C. Taupin, M. Dvolaitzky, C. Sauterey, *Biochemistry*, 1975, **14**, 4771-4775.
16. B. V. Deryagin, Y. V. Gutop, *Kolloidn. Zh*. (rus), 1962, **24**, 370- 374.
17. M. A. S. Karal, M. Yamazaki, *J. Chem. Phys*., 2015, **143**, 081103.
18. Y. Tamba, H. Terashima, M. Yamazaki, M. *Chem*. *Phys*. *Lipids*, 2011, **164**, 351-358.
19. M. Yamazaki, *Adv. Planar Lipid Bilayers and Liposomes*, 2008, **7**, 121-142.
20. W. Rawictz, K. C. Olbrich, T. McIntosh, D. Needham, E. Evans, *Biophys. J*. 2000**, 79**, 328-339.

21. J. Wohlert, W. K. den Otter, O. Edholm, W. J. Briels, *J. Chem. Phys.* 2006, **124**, 154905.
22. D. P. Tieleman, H. Leontiaudou, A. E. Mark, S.-J. Marrink, *J. Amer. Chem. Soc*. 2003, **125**, 6382-6383.
23. E. J. W. Verway, J. Th. G. Overbeek, Theory of the stability of lyophobic colloids, Elsevier, Amsterdam, 1948.
24. J. N. Israelachvili, Intermolecular and surface forces*,* 2nd ed. Academic Press, New York, 1992.
25. M. Zasloff, *Nature,* 2002, **415**, 389-395.
26. S. McLaughlin, D. Murray, *Nature*, 2005, **438**, 605-611.
27. S. J. Li. Y. Yamashita, M. Yamazaki, *Biophys. J.*, 2001, **81**, 983-993.
28. Y. Tamba, M.Yamazaki, *J. Phys. Chem. B*, 2009, **113**, 4846-4852.
29. J. F. Nagle, S. Tristram-Nagle, *Biochim. Biophys. Acta*, 2000**, 1469**, 159-195.
30. M. Fošnarič, V. Kralj-Iglič, B.K. Bohinc, S. May, *J. Phys. Chem. B*, 2003, **107**, 12519-12526.
31. M. D. Betterton, M. P. Brenner, *Phys. Rev. Lett.* 1999, **82**, 1598-1601.
32. H. N. W. Lekkerkerker, Physica A, 1989, **159**, 319-328.
33. R. W. Glaser, S. L. Leikin, L. Chernomordik, V. F. Pastushenko, A. I. Sokirko, *Biochim. Biophys. Acta*, 1988, **940**, 275-287.
34. T. V. Tolpekina, W. K. den Otter, W. J. Briels, *J. Chem. Phys.* 2004, **121**, 12060-12066.
35. Z. –J. Wang, D. Frenkel, *J. Chem. Phys.* 2005**, 123**, 154701.
36. T. Oka, T. Saiki, J. M. Alam, M. Yamazaki, *Langmuir*, 32, 1327-1337, 2016.
37. P. Hänggi, P. Talkner, M. Borkovec, *Rev. Mod. Phys.* 1990, **62**, 251-341.
38. C. W. Gardiner, Handbook of Stochastic Methods for Physics, Chemistry, and the Natural Sciences, Springer-Verlag, Berlin, 1990.
39. N. G. van Kampen, Stochastic processes in physics and chemistry, 3rd ed., North Holland, 2007.
40. J. P. Slotte, *Biochim. Biophys. Acta*, 2016, **1858**, 304-310.

Table 1: k_p values for 40%DOPG/60%DOPC-GUVs at various tension and temperature

σ (mN/m)	T (°C)	k_p (s^{-1})
7.0	12	$(6.7 \pm 0.3) \times 10^{-3}$
	18	$(9.0 \pm 0.5) \times 10^{-3}$
	25	$(1.5 \pm 0.1) \times 10^{-2}$
6.0	20	$(3.7 \pm 0.1) \times 10^{-3}$
	25	$(4.8 \pm 0.2) \times 10^{-3}$
	30	$(6.6 \pm 0.2) \times 10^{-3}$
5.0	25	$(1.9 \pm 0.2) \times 10^{-3}$
	32	$(3.1 \pm 0.2) \times 10^{-3}$
	37	$(4.4 \pm 0.1) \times 10^{-3}$

Table 2: Dependence of U_0 and Γ on a (or B) values at 25 °C

The values of parameters were determined by the fitting in Fig. 2.

a	B (mN/m)	U_0 (pN·nm)	Γ (pN)
0.56	0.2	23 ± 9	10 ± 2
0.54	0.6	18 ± 9	11 ± 2
0.51	1.3	12 ± 11	12 ± 2
0.49	1.8	9.0 ± 0.4	12.4 ± 0.2
0.47	2.2	5 ± 12	13 ± 2
0.45	2.6	3 ± 12	14 ± 2

Table 3: Activation energy, U_a, at various temperature

The U_a value for each temperature was obtained using eq. 6 and the best fit parameters (a = 0.49, U_0 = 9.0 pN·nm, Γ = 12.4 pN)

σ (mN/m)	T (°C)	B (mN/m)	(σ+B) (mN/m)	U_a (pN·nm)
7.0	12	1.5	8.5	66
	18	1.6	8.6	65
	25	1.8	8.8	64
6.0	20	1.7	7.7	72
	25	1.8	7.8	71
	30	1.9	7.9	70
5.0	25	1.8	6.8	81
	32	1.9	6.9	79
	37	2.1	7.1	78

Figure Legends

Fig. 1. Temperature effect on tension-induced rupture in a single 40%DOPG/60%DOPC-GUV. (A) Time-course of $P_{intact}(t)$ for σ = 7.0 mN/m at 12 °C (○), 18 °C (▲), and 25 °C (□). The solid lines represent the best-fit curve for eq. 2. (B) Relationship between ln k_p and $1/T$ for σ = 5.0 mN/m (green □), 6.0 mN/m (red Δ), and 7.0 mN/m (○). Average values and standard error (shown by error bars) of k_p for each temperature were determined in three independent experiments, each using 20 GUVs. The solid line shows the best-fit linear line.

Fig. 2. Tension dependence of U_a of the rupture of the GUVs. Relationship between U_a and $1/(\sigma + B)$ at 25 °C is shown. The solid line shows the best fit to eq. 6.

Fig. 3. Fitting of the data of the tension dependence of k_p at 25 °C using the Arrhenius equation. (□) 40%DOPG/60%DOPC- and (○) DOPC-GUV. Mean values and standard error of k_p for each tension are shown. These data are reprinted from Ref. 11 with permission from the American Chemical Society. The solid lines show the best fits to the theoretical curves corresponding to eq. 7 using $A_F = 5.0 \times 10^4$ (s^{-1}) for 40%DOPG/60%DOPC-GUV (blue line), and $A_F = 6.3 \times 10^5$ (s^{-1}) for DOPC-GUV (red line).

Fig. 4. Illustration of a hydrophilic pre-pore and its free energy profile as a function of pre-pore radius, r. (A)(1) State I between a hydrophobic rarefaction and a hydrophilic pre-pore at $r = r_0$. (2) A hydrophilic pre-pore with radius of r. (B) Illustration of the free energy of a hydrophilic pre-pore as a function of its pre-pore radius, r.

Fig. 5. Two kinds of free energy profile of a pre-pore as a function of pre-pore radius, r. (A) Model A has an energy barrier between the intact and intermediate states. (B) Model B has no energy barrier between the two states.

Fig. 1

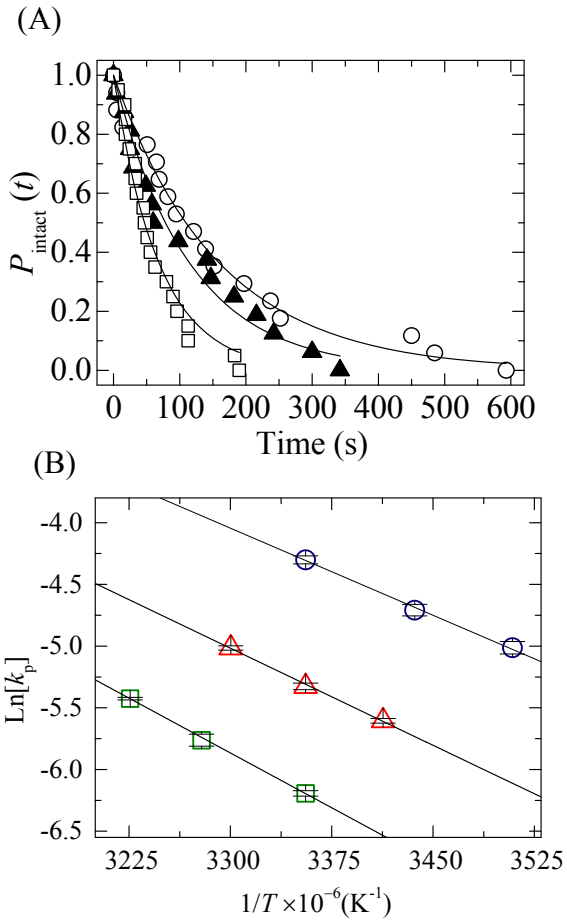
(A)
1.0
0.8
0.6
0.4
0.2
0.0
$P_{intact}(t)$
0
100
200
300
400
500
600
Time (s)
(B)
-4.0
-4.5
-5.0
-5.5
-6.0
-6.5
Ln[k_p]
3225
3300
3375
3450
3525
$1/T \times 10^{-6}(K^{-1})$

Fig. 2

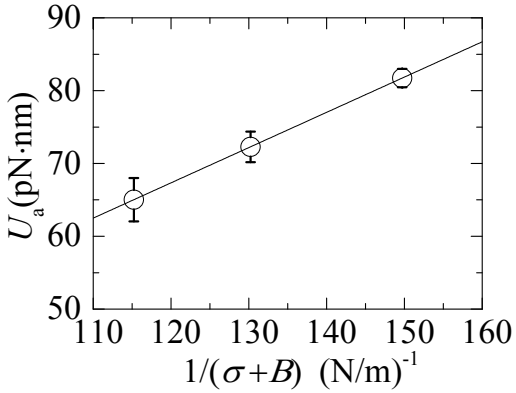

Fig. 3

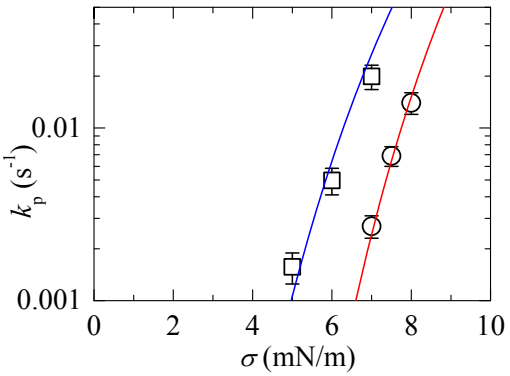

Fig.4

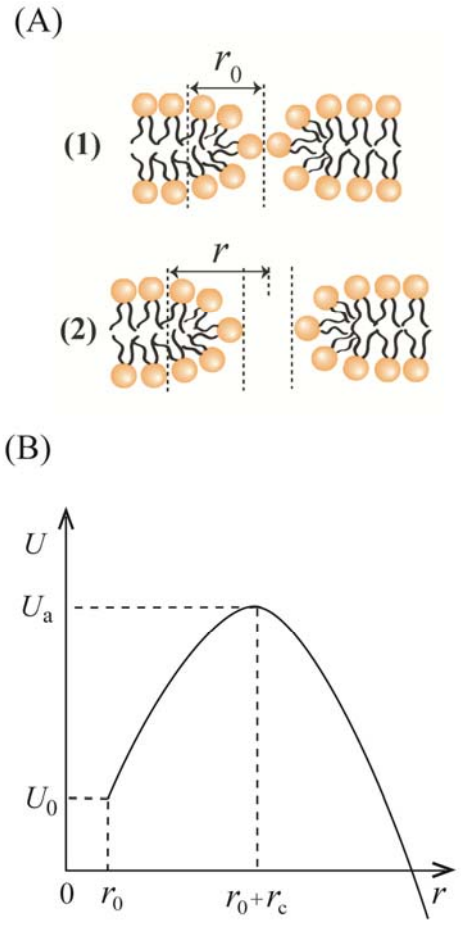

Fig. 5